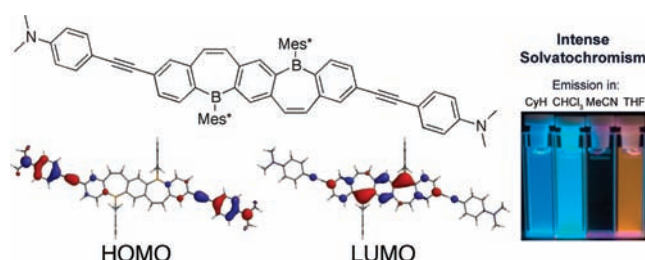


Conjugated “B-Entacenes”: Polycyclic  
Aromatics Containing Two Borepin RingsAnthony Caruso Jr.<sup>†</sup> and John D. Tovar<sup>\*,†,‡</sup>Department of Chemistry and Department of Materials Science and Engineering,  
Johns Hopkins University, Baltimore, Maryland 21218, United States

tovar@jhu.edu

Received April 16, 2011

## ABSTRACT



The synthesis and characterization of functionalized bora-acenes (B-entacenes) where Stille and Sonogashira cross-couplings were used to attach a series of electron-donating and -withdrawing substituents is reported. Photophysical, electrochemical, and computational analyses revealed that the LUMO level can be tuned by changing the *para*-conjugated substituent. Furthermore, the dimethylamino-functionalized molecule exhibited intense solvatochromism due to the intramolecular charge-transfer interaction.

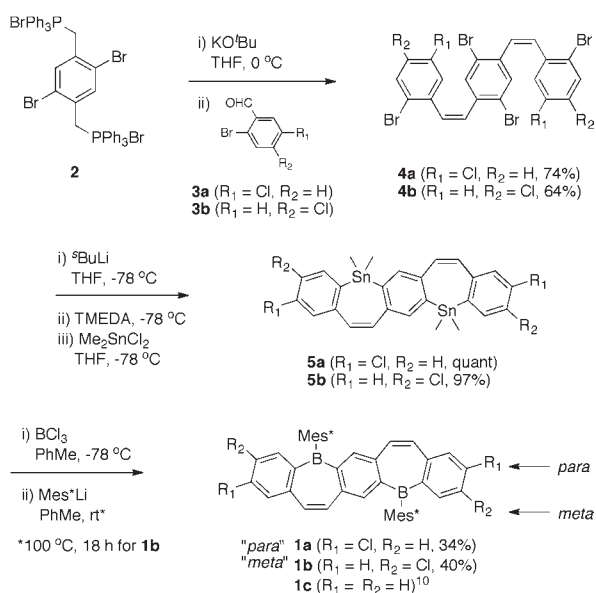
In the search for new organic electronic materials, acenes and heteroacenes have become leading candidates for replacing amorphous silicon and other inorganics in systems that require low cost, highly tunable and easily processable materials for applications such as thin film transistors (TFTs),<sup>1</sup> sensors<sup>2</sup> and photovoltaics.<sup>3</sup> In fact, in some areas pentacene already rivals the performance of amorphous silicon.<sup>4</sup> To date, the majority of acenes and heteroacenes synthesized and studied have been p-channel (hole-transporting) semiconductors. Progress has been made in preparing n-channel (electron-transporting)

materials based on acene-like platforms. Anthony<sup>5</sup> and Bao<sup>6</sup> have independently reported the functionalization of thienoacenes, pentacenes, and perylene diimides with electron-deficient groups as a method of increasing the electron-transporting ability of these materials. Bunz and co-workers systematically replaced carbons in the acene backbone with heteroatoms (specifically nitrogen) resulting in hole- and electron-transporting materials.<sup>7</sup> There remains a need for new electron-transporting materials because of the difficulty in synthesizing air-stable n-channel semiconductors in their doped forms.

<sup>†</sup> Department of Chemistry.<sup>‡</sup> Department of Materials Science and Engineering.(1) (a) Pisula, W.; Feng, X.; Mullen, K. *Chem. Mater.* **2011**, *23*, 554–567. (b) Jung, B. J.; Lee, K.; Sun, J.; Andreou, A. G.; Katz, H. E. *Adv. Funct. Mater.* **2010**, *20*, 2930–2944.(2) Khan, H. U.; Roberts, M. E.; Knoll, W.; Bao, Z. *Chem. Mater.* **2011**, *23*, 1946–1953.(3) Facchetti, A. *Chem. Mater.* **2011**, *3*, 733–758. (b) Brunetti, F. G.; Gong, X.; Tong, M.; Heeger, A. J.; Wudl, F. *Angew. Chem., Int. Ed.* **2010**, *49*, 532–536. (c) Gorodetsky, A. A.; Cox, M.; Tremblay, N. J.; Kymissis, I.; Nuckolls, C. *Chem. Mater.* **2009**, *21*, 4090–4092. (d) Ling, M. M.; Erk, P.; Gomez, M.; Koenemann, M.; Locklin, J.; Bao, Z. *Adv. Mater.* **2007**, *19*, 1123–1127.(4) (a) Halik, M.; Klauk, H.; Zschieschang, U.; Schmid, G.; Dehm, C.; Schutz, M.; Maisch, S.; Effenerger, F.; Brunnbauer, M.; Stellacci, F. *Nature* **2004**, *431*, 963–966. (b) Dimitrakopoulos, C. D.; Malenfant, P. R. L. *Adv. Mater.* **2002**, *14*, 99–117. (c) Lin, Y. Y.; Gundlach, D. J.; Nelson, S. F.; Jackson, T. N. *IEEE Trans. Electron Devices* **1997**, *44*, 1325.(5) (a) Anthony, J. E.; Facchetti, A.; Heeney, M.; Marder, S. R.; Zhan, X. *Adv. Mater.* **2010**, *22*, 3876–3892. (b) Swartz, C. R.; Parkin, S. R.; Bullock, J. E.; Anthony, J. E.; Mayer, A. C.; Malliaras, G. G. *Org. Lett.* **2005**, *7*, 3163–3166.(6) (a) Okamoto, T.; Nakahara, K.; Saeki, A.; Seki, S.; Oh, J. H.; Akkerman, H. B.; Bao, Z.; Matsuo, Y. *Chem. Mater.* **2011**, *23*, 1946–1953. (b) Tang, M. L.; Oh, J. H.; Reichardt, A. D.; Bao, Z. *J. Am. Chem. Soc.* **2009**, *131*, 3733–3740. (c) Tang, M. L.; Okamoto, T.; Bao, Z. *J. Am. Chem. Soc.* **2006**, *128*, 16002–16003.(7) (a) Wu, J. I.; Wannere, C. S.; Mo, Y.; Schleyer, P. v. R.; Bunz, U. H. F. *J. Org. Chem.* **2009**, *74*, 4343–4349. (b) Miao, S.; Appleton, A.; Berger, N.; Barlow, S.; Marder, S. R.; Hardcastle, K. I.; Bunz, U. H. F. *Chem.—Eur. J.* **2009**, *15*, 4990–4993.(8) (a) Wakamiya, A.; Mori, K.; Araki, T.; Yamaguchi, S. *J. Am. Chem. Soc.* **2009**, *131*, 10850–10851. (b) Wakamiya, A.; Mishima, K.; Ekawa, K.; Yamaguchi, S. *Chem. Commun.* **2008**, 579–581. (c) Yamaguchi, S.; Wakamiya, A. *Pure Appl. Chem.* **2006**, *78*, 1413–1424. (d) Yamaguchi, S.; Shirasaka, T.; Akiyama, S.; Tamao, K. *J. Am. Chem. Soc.* **2002**, *124*, 8816–8817.

The insertion of neutral, planar boron centers, which are inherently electron deficient, into polycyclic aromatic frameworks has been less developed. For example, Yamaguchi,<sup>8</sup> Perepichka,<sup>9</sup> and we recently inserted boron centers into  $\pi$ -conjugated systems such as diborins, azaborine–thiophene heteroacenes, and borepins, respectively. The borepins displayed well-behaved cathodic electrochemistry at the boron centers, which is useful for n-channel and NLO materials. Herein, we report the synthesis of extended fused polycyclic aromatics containing two formally aromatic borepin rings and the study of a series of functionalized systems with electron-donating, -withdrawing, and -neutral substituents. We refer to these systems as “*B*-entacenes” because they are boron-containing pentacyclic acenes.

**Scheme 1.** Synthesis of *Para*- and *Meta*-Chlorinated *B*-Entacenes



We previously reported chlorinated *B*-entacene **1a**<sup>10</sup> but found that only nickel-catalyzed cross-couplings of aryl Grignards were able to functionalize the polycyclic core. Subsequently, Buchwald conditions using the Pd(MeCN)<sub>2</sub>Cl<sub>2</sub>/XPhos catalyst<sup>11</sup> were used by Piers to enable palladium-catalyzed reactions with chlorinated dibenzo[*b,f*]silepins.<sup>12</sup> Thus, we revisited the reactivity of **1a** and sought to extend this to the *meta* isomer **1b**, prepared as shown in Scheme 1. The bis(phosphonium salt) **2**<sup>13</sup> was

used as a common core from which double Wittig olefinations with bromochlorobenzaldehyde **3b** resulted in the *meta*-chlorinated tetrabromide **4b**. Chemoselective lithium–halogen exchange with the bromides followed by in situ treatment of the tetralithio species with 2 equiv of dimethyltin dichloride yielded fused stannepin **5b**. Tin–boron exchanges between boron trichloride and the dimethyltin centers of **5b** followed by treatment with Mes\*Li (Mes\* = 2,4,6-tri-*tert*-butylphenyl) provided **1b** in 40% yield.

Table 1 shows the functionalized borepins accessible with more active palladium-catalyzed cross-coupling conditions. Stille coupling between **1a** and 2-tributylstannylthiophene using Fu's Pd(P-*t*-Bu<sub>3</sub>)<sub>2</sub> catalyst<sup>14</sup> resulted in *p*-thienyl *B*-entacene **6a** in 34% yield. The transformation was quantitative by crude <sup>1</sup>H NMR; however, purification of these compounds often resulted in lower isolated yields because of poor solubility. Sonogashira couplings under Buchwald conditions resulted in a series of *para*-substituted phenylethynyl *B*-entacenes **6b–f**. The series included electron-withdrawing 4-ethyl ester phenylacetylene and 4-fluorophenylacetylene, neutral phenylacetylene, and electron-donating anisole and *N,N*-dimethylaminophenylacetylene *B*-entacenes. The molecules were thermally robust up to their melting points in DSC (see Figures S26–28, Supporting Information).

Unexpectedly, the *meta*-chlorinated *B*-entacene **1b** would not react under several variations of active palladium cross-coupling conditions, resulting in the isolation of starting material in each case. As a result, **1b** was subjected to Kumada coupling conditions using Ni(dppp)Cl<sub>2</sub>, which is known to be more reactive toward chlorides; however, to our surprise no reaction occurred. A lack of reactivity of the *meta* chloride *B*-entacene **1b** was unforeseen since we previously reported the functionalization of *meta* bromide DBBs by common cross-coupling procedures.<sup>15</sup> For this reason, electronic factors arising from the inductive effects of the more electron-deficient *p*-diphenylene diborane are thought to be the barrier preventing successful cross-couplings and not steric encumbrance.

Figure 1a shows representative electronic spectra for the *p*-phenylethynyl *B*-entacenes (data for all measurements are compiled numerically in Tables 2 and S2, Supporting Information). Borepins **6a,c–f** showed low energy bands of low oscillator strength at ca. 445 nm attributed to charge-transfer between the appended electron-rich handle and the electron-deficient boron center. Intense  $\pi-\pi^*$  transitions were observed, some with structured vibronic features at higher energy. Not surprisingly, the stronger dimethylamino phenylacetylene donor substituent appended to the *B*-entacene (**6b**) had a much more intense but ill-defined low energy absorption. The photoluminescence

(9) Lepeltier, M.; Lukoyanova, O.; Jacobson, A.; Perepichka, D. F. *Chem. Commun.* **2010**, 46, 7007–7009.

(10) Caruso, A.; Siegler, M. A.; Tovar, J. D. *Angew. Chem., Int. Ed.* **2010**, 49, 4213–4217.

(11) Gelman, D.; Buchwald, S. L. *Angew. Chem., Int. Ed.* **2003**, 42, 5993–5996.

(12) Mercier, L. G.; Furukawa, S.; Piers, W. G.; Wakamiya, A.; Yamaguchi, S.; Parvez, M.; Harrington, R. W.; Clegg, W. *Organometallics* **2011**, 30, 1719–1729.

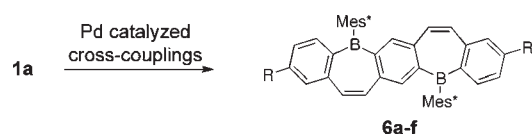
(13) Bonifacio, M. C.; Robertson, C. R.; Jung, J. Y.; King, B. T. *J. Org. Chem.* **2005**, 70, 8522–8526.

(14) Littke, A. F.; Schwarz, L.; Fu, G. C. *J. Am. Chem. Soc.* **2002**, 124, 6343–6348.

(15) Caruso, A., Jr.; Tovar, J. D. *J. Org. Chem.* **2011**, 76, 2227–2239.

(16) Swager, T. M.; Gil, C. J.; Wrighton, M. S. *J. Phys. Chem.* **1995**, 99, 4886–4893.

**Table 1.** Palladium-Catalyzed Cross-Couplings of *Para*-Chlorinated *B*-Entacene **1a**<sup>a</sup>



product	conditions	R-	yield <sup>a</sup>
<b>6a</b>	<b>a</b>		23% <sup>b</sup>
<b>6b</b>	<b>b</b>		quant
<b>6c</b>	<b>b</b>		50% <sup>b</sup>
<b>6d</b>	<b>b</b>		34% <sup>b</sup>
<b>6e</b>	<b>b</b>		quant
<b>6f</b>	<b>b</b>		34%

<sup>a</sup> Isolated yields. <sup>b</sup> Quantitative by <sup>1</sup>H NMR. <sup>a</sup> Conditions: (a) Pd<sub>2</sub>(dba)<sub>3</sub>/P(<sup>t</sup>Bu)<sub>3</sub>, dioxane, CsF, 100 °C; (b) Pd(MeCN)<sub>2</sub>Cl<sub>2</sub>/XPhos, Cs<sub>2</sub>CO<sub>3</sub>, MeCN, THF, heat.

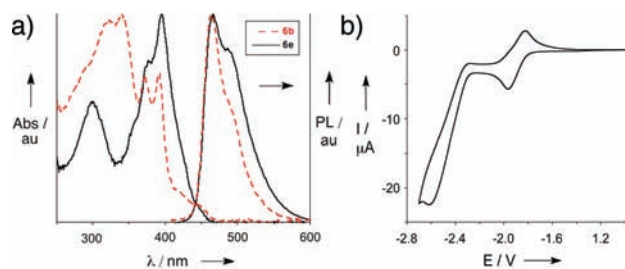


**Figure 1.** UV–vis and PL spectra (a) for **6b,e** (acquired in CHCl<sub>3</sub> at room temperature with excitation at 392 nm) and CV of **6b** (b) (2 mM acquired in 0.1 M *n*-Bu<sub>4</sub>NPF<sub>6</sub>/THF and reported relative to Ag/Ag<sup>+</sup>).

(PL) spectra of the *B*-entacenes **6a–f** were bimodal with a more intense higher energy  $\lambda_{\max}$  at ca. 464 nm and a less intense low energy shoulder. Time-resolved photoluminescence on the *B*-entacenes revealed single exponential decays with lifetimes between 6.8 and 9.6 ns with no noticeable trends. We did not observe significant spectral differences regardless of substituent electronics. We attribute this to the node present in the wave function at the site of attachment to the *B*-entacene core preventing delocalization of the frontier molecular orbital surfaces (see the Supporting Information).

Figure 1b shows a representative cyclic voltammogram (CV) for the reductions of **6b**. The first reduction half-wave potential ( $E_{1/2}$ ) was  $-1.93$  V, while the second process was ca. 600 mV more negative. All of the functionalized *B*-entacenes exhibited similar cathodic electrochemistry with two one-electron reductions; furthermore, the electron-rich *B*-entacenes **6a–c** were more difficult to reduce than the neutral and electron-deficient *B*-entacenes **6d–f**. In addition to the well-behaved nature of these cathodic processes, the ability to tune the LUMO level by changing the functional handle *para* to the boron center (e.g.,  $-2.76$  to  $-3.08$  eV) could enable the fashioning of *B*-entacene into electron-accepting materials via substituent fine-tuning.

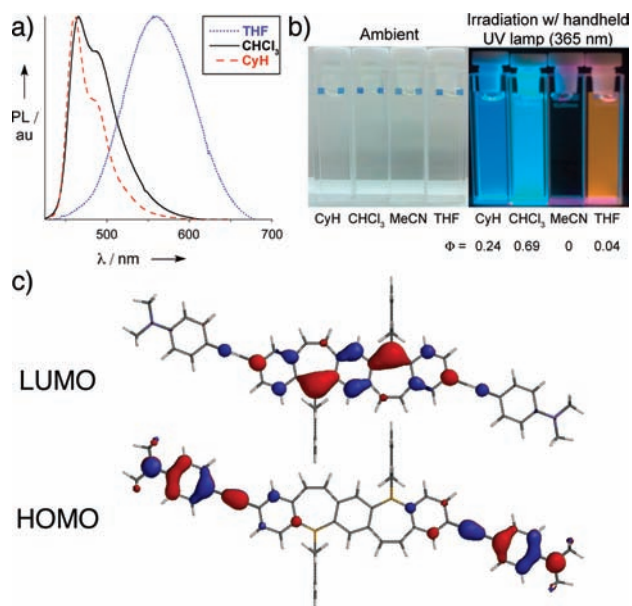
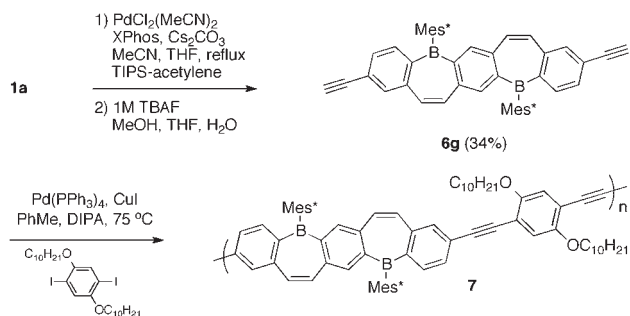


**Figure 2.** PL spectra for **6b** in various solvents (a) (acquired at room temperature, with excitation at 392 nm), image of solutions without (left) and with (right) irradiation with hand-held UV (365 nm) (b) and DFT (B3LYP/6-31G\*) calculations of the LUMO (top) and HOMO (bottom) surfaces (c).

The PL spectra of the *B*-entacenes with electron-donating groups **6b–c** were also acquired in solvents with different  $E_T30$  values in order to see if there were any solvatochromic effects due to the “push-pull” electronic character. The methoxy donor **6c** showed no more than a 6 nm shift in going from nonpolar to polar solvents (see Figure S15, Supporting Information); however, the dimethylamino donor **6b** showed a shift of nearly 100 nm (see Figure 2a,b). DFT calculations (B3LYP/6-31G\*) rationalized this behavior by revealing a large shift in orbital density between the HOMO and LUMO surface for **6b** (Figure 2c), while the HOMO and LUMO wave functions are predominantly localized on the *B*-entacene core for **6c** (see Figure S20, Supporting Information).

The ability to perform Sonogashira couplings on **1a** allowed for the synthesis of *p*-TIPS-ethynyl substituted *B*-entacenes that could be deprotected by treatment with

## Scheme 2. Sonogashira Polymerization Leading to 7



tetrabutylammonium fluoride to provide the terminal alkyne **6f** in 34% yield over two steps as shown in Scheme 2. This alkyne was then polymerized under standard Sonogashira conditions with bis(decyloxy)-2,5-diiodobenzene<sup>16</sup> to form polymer **7** in 70% yield ( $M_n$  4400, PDI 1.60). This oligomeric material was readily dissolved in common organic solvents such as chloroform and toluene, which would allow for solution processability.

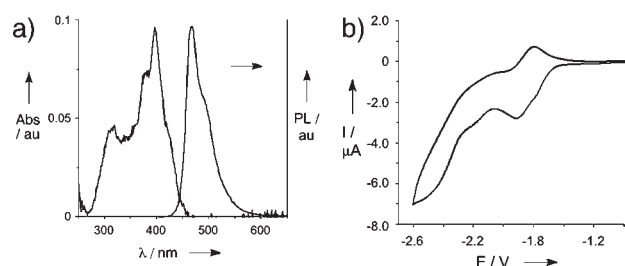


**Figure 3.** UV-vis, PL (a) and CV (b) data for **7**. UV-vis and PL spectra were acquired in  $\text{CHCl}_3$  at room temperature with excitation at 399 nm, CV acquired in 0.1 M  $n\text{-Bu}_4\text{NPF}_6/\text{THF}$  and reported relative to  $\text{Ag}/\text{Ag}^+$ .

Polymer **7** had an onset of absorption at 459 nm and a more intense higher energy band at 396 nm. The typical lower energy, low oscillator strength bands associated with a charge-transfer interaction were more intense, but overlapping with the  $\pi$ - $\pi^*$  transition. PL spectra for **7** showed a peak at 466 nm that had a low energy shoulder at 490 nm and a quantum yield of 45% (Figure 3a). The CV spectrum of **7** showed two reductions ( $E_{1/2} = -1.86, -2.37$  V) that were more broad than those seen for the monomers (Figure 3b). The photophysical and electrochemical data for **7** were quite similar to those for related dibenzoborepin polymers<sup>15</sup> and suggested that **7** behaved like an

alkynylated monomer with localized electronic structure rather than an extended system with any sort of long-range communication between the oligomeric *B*-entacenes as witnessed by the localized HOMO and LUMO surfaces of the *B*-entacenes (see the Supporting Information) with the exception of **6b**. The inherent electronic structure of this *B*-entacene pathway is thus restricted relative to other  $\pi$ -conjugated polymers.

**Table 2.** Summary of Photophysical and Electrochemical Data

compd	abs $\lambda_{\text{onset}}$ (nm)	PL $\lambda_{\text{max}}$ (nm)	$\Phi$	$\tau^a$ (ns)	$E_{1/2}^b$ (V)
<b>1c</b> <sup>11</sup>	458	456	0.71	9.3	-1.89, -2.46
<b>6a</b>	459	460	0.36	7.3	-1.99, -2.52
<b>6b</b>	462	465	0.69	6.8	-1.93, -2.49
<b>6c</b>	463	463	0.52	9.2	-1.85, -2.62
<b>6d</b>	466	465	0.45	8.9	-1.89, -2.38
<b>6e</b>	471	464	0.29	9.1	-1.84, -2.34
<b>6f</b>	467	465	0.49	9.6	-1.83, -2.22
<b>7</b>	459	466	0.45	8.6	-1.86, -2.37

<sup>a</sup>All lifetimes are single exponential. <sup>b</sup> $E_{1/2}$ 's are reported relative to  $\text{Ag}/\text{Ag}^+$  with which the  $\text{Fc}/\text{Fc}^+$  couple was found to be 205 mV.

This report describes the synthesis of *para*- and *meta*-chlorinated *B*-entacenes and the subsequent functionalization of the *para* system by Stille and Sonogashira cross-coupling reactions. With an expanded cross-coupling repertoire, we were able to synthesize a series of electron-donating, -withdrawing, and -neutral groups appended to the electron-accepting *B*-entacenes cores. Optical and electrochemical characterization revealed that the band gap remains quantitatively the same, as seen by the similar  $\lambda_{\text{onset}}$ s of absorption for **6a–f**, while the LUMO was tuned by changing the electronic character of the conjugated substituent. Electron-deficient acceptor materials in which the energy levels can be tuned to optimize interactions with electron-rich donor materials are of great interest for future work with heterostructures or blends for use in organic device fabrication.

**Acknowledgment.** We thank Johns Hopkins University for generous support. A.C. was supported by a JHU Chemistry Alumni Graduate Fellowship.

**Supporting Information Available.** Experimental details, characterization data, and molecular orbital surfaces. This material is available free of charge via the Internet at <http://pubs.acs.org>.